

THE MID-INFRARED SPECTRUM REVISITED

F. GALLIANO

May 28, 2010

Contents

1 Fine Tuning the Method	1
1.1 Line Fitting	1
1.2 Continuum and Resolved Feature Fitting	4
1.3 Calibration of the Aromatic Feature Profiles	5
2 Application	12
2.1 The Calling sequence	12
2.2 Error Analysis	12
References	12

1 Fine Tuning the Method

MILES (Mid-Infrared Line Extraction Software; [Galliano et al., 2010](#)) performs the fit of mid-IR spectra in two parts:

1. Atomic and molecular unresolved line fitting (one by one);
2. Dust continuum, aromatic bands, foreground extinction (dust and ices) and stellar contamination (everything at the same time).

1.1 Line Fitting

The line fitting is done on each line separately, since they are unresolved. For each line i (Table 1), we assume a Gauss profile and second order polynomial baseline:

$$F_\nu^{\text{line}}(\nu; i) = \frac{I_{\text{line}}(i)}{\sqrt{2\pi}\sigma(i)} \times \exp\left[-\frac{(\nu - \nu_0(i))^2}{2\sigma(i)^2}\right] + a(i) \times \left[1 + b(i)\left(\frac{\nu}{\nu_0(i)} - 1\right) + c(i)\left(\frac{\nu}{\nu_0(i)} - 1\right)^2\right], \quad (1)$$

where the parameters are:

1. The integrated line intensity, $I_{\text{line}}(i)$, which is free to vary;
2. The line central frequency $\nu_0(i)$ (Table 1), which is either fixed or free to vary by $\pm 1/2$ pixel;
3. The line width, $\sigma(i)$, either fixed to the instrumental resolution $\sigma_{\text{inst}}(i)$, or free to vary between $\sigma_{\text{inst}}(i)/2$ and $2\sigma_{\text{inst}}(i)$.
4. The three baseline parameters $a(i)$, $b(i)$, $c(i)$.

Fig. 1 shows the fits of the lines for the 5-20 μm SWS spectrum of NGC 7027 ([Bernard Salas et al., 2001](#)). These line templates are then added (fixed) to the other components to fit the total spectrum.

Central wavelength [μm]	Species and Transition	Input Code Label
5.1286570	H I 6-10	H I 6-10
5.5111600	H ₂ 0-0 S(7)	H2S7
5.6098000	[Mg V] 3P ² -3P ¹	MgV
5.9082130	Humphreys γ	Huc
5.9810000	[K IV]	KIV
6.1085600	H ₂ 0-0 S(6)	H2S6
6.7090000	[Cl V] 2P ⁰ -2P ⁰	ClV
6.9095200	H ₂ 0-0 S(5)	H2S5
6.9479840	He II 8-9	HeIII1
6.9852740	[Ar II] 2P ^{3/2} -2P ^{1/2}	ArII
7.3178000	[Na III] 2P ⁰ -2P ⁰	NaIII
7.4598580	Pfund α	Pfa
7.5024930	Humphreys β	Hub
7.6524000	[Ne VI] 2P ⁰ -2P ⁰	NeVI
7.8145000	[Fe sc vii] 3F ³ -3F ⁴	FeVII
7.9015800	[Ar V] 3P ¹ -3P ²	ArV
8.0250500	H ₂ 0-0 S(4)	H2S4
8.7600640	H I 7-10	H I 7-10
8.9910300	[Ar III] 3P ² -3P ¹	ArIIII1
9.0420000	[Ni VI] 4P ^{5/2} -4F ^{5/2}	NiVI
9.5267000	[Fe VII] 3F ² -3F ³	FeVII
9.6649100	H ₂ 0-0 S(3)	H2S3
9.7134750	He II 9-10	HeII2
10.338500	[Si I] 1P ¹ -1P ²	SiI
10.510500	[S IV] 2P ^{3/2} -2P ^{1/2}	SIV
12.278610	H ₂ 0-0 S(2)	H2S2
12.368527	Humphreys α	Hua
12.813550	[Ne II] 2P ^{3/2} -2P ^{1/2}	NeII
13.102190	[Ar V] 3P ⁰ -3P ¹	ArV
13.521000	[Mg V] 3P ¹ -3P ⁰	MgV
14.321680	[Ne V] 3P ¹ -3P ²	NeV1
15.555000	[Ne III] 3P ² -3P ¹	NeIIII1
17.034830	H ₂ 0-0 S(1)	H2S1
17.608246	H I 11-18	H I 11-18
18.712900	[S III] 3P ² -3P ¹	SIII1
19.061898	H I 7-8	H I 7-8
21.829100	[Ar III] 3P ¹ -3P ⁰	ArIIII2
24.317500	[Ne V] 3P ⁰ -3P ¹	NeV2
25.890300	[O IV] 2P ^{3/2} -2P ^{1/2}	OIV
28.218830	H ₂ 0-0 S(0)	H2S0
33.481000	[S III] 3P ¹ -3P ⁰	SIII2
34.815200	[Si II] 2P ^{3/2} -2P ^{1/2}	SiII
35.349100	[Fe II] 6D ^{5/2} -6D ^{7/2}	FeII2
36.013500	[Ne III] 3P ¹ -3P ⁰	NeIIII2

Table 1: Atomic and molecular line list.

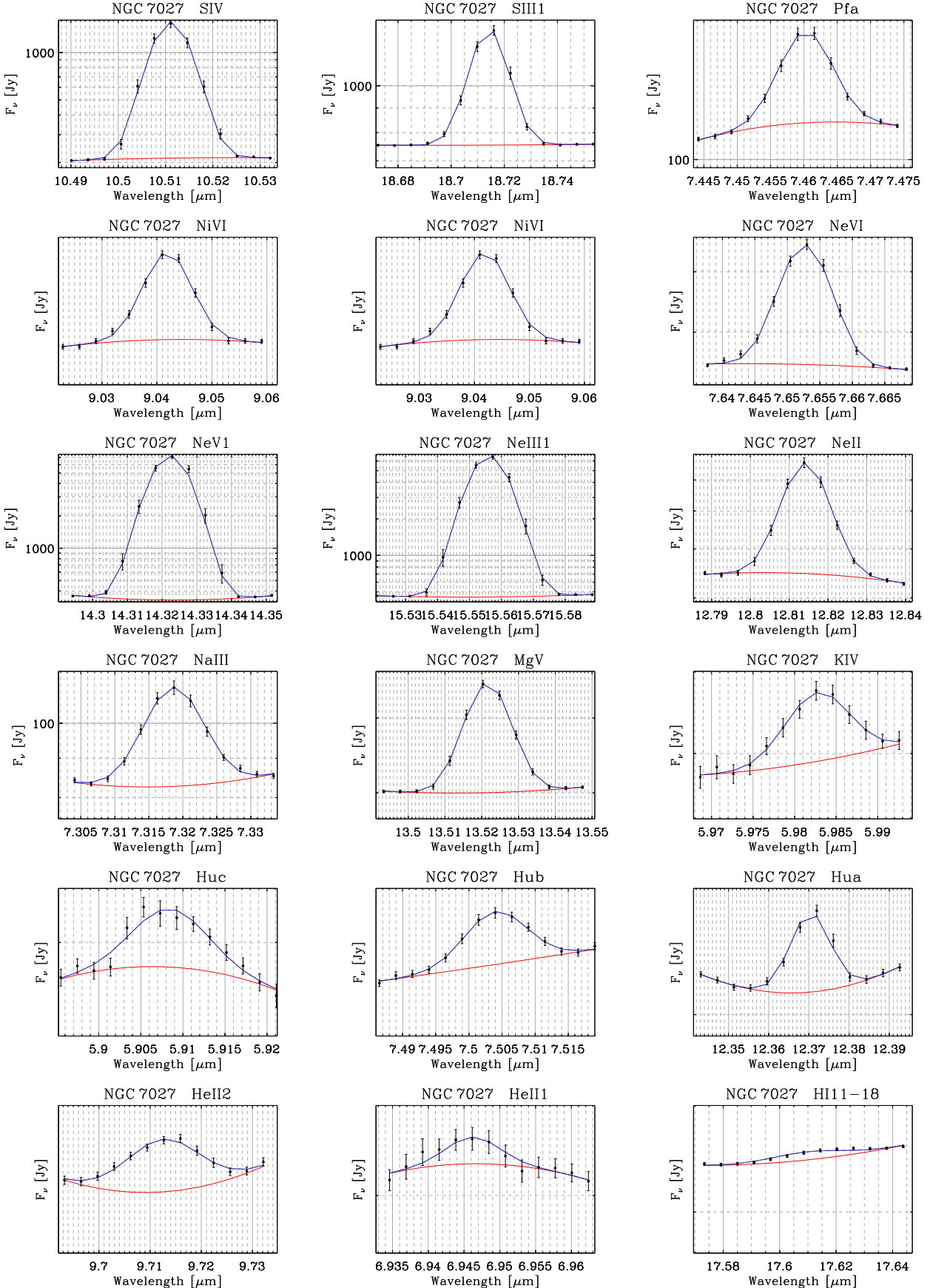


Figure 1: Select individual line fits of the SWS spectrum of NGC 7027.

1.2 Continuum and Resolved Feature Fitting

Then the fit of the other components is done simultaneously since they combine in a non-linear way. The components are the followings.

1. The fitted line template (Eq. 1), which is fixed to:

$$F_\nu^{\text{line}}(\nu) = \sum_{i=1}^{N_{\text{line}}} F_\nu^{\text{line}}(\nu; i). \quad (2)$$

2. The stellar continuum, to account for old contamination of old stellar populations or the tail of young stars close to the source, $F_\nu^*(\nu)$. It is modeled by a single burst with PEGASE (Fioc & Rocca-Volmerange, 1997), at 5 Gyr. Since we fit only the Rayleigh-Jeans slope ($\lambda \gtrsim 5 \mu\text{m}$), those parameters do not matter. This component is simply scaled up and down. This component is controlled by a single parameter M_* .
3. The dust grain continuum is the linear combination of N_{grain} modified blackbodies, with temperatures $T(i)$ and masses $M(i)$ free to vary, and realistic absorption opacities $Q_{\text{abs}}(\nu; i)$ and specific volume $\rho(i)$ (Table 2):

$$F_\nu^{\text{grain}}(\nu; i) = \frac{M(i)}{d^2} \frac{3}{4\rho(i)} \left(\frac{Q_{\text{abs}}(\nu; i)}{a} \right) B_\nu(T(i); \nu). \quad (3)$$

Component	Reference	Input Code Label
Graphite	Laor & Draine (1993)	gra
Amorphous carbon (BE)	Rouleau & Martin (1991)	crb
Silicate	Jäger et al. (2003)	sil_norm
Astronomical silicate	Weingartner & Draine (2001)	sil
Corundum	Begemann et al. (1997)	al2o3_compact
Astronomical corundum	Koike et al. (1995)	al2o3_koike

Table 2: Set of grain opacities.

4. The aromatic bands are modeled with asymmetric Lorentz profiles, in order to account for the anharmonicity:

$$F_\nu^{\text{band}}(\nu) = I_{\text{band}}(i) \times \begin{cases} \frac{2}{1 + \Delta\nu_{\text{long}}(i)/\Delta\nu_{\text{short}}(i)} \frac{\Delta\nu_{\text{short}}(i)}{\pi} \frac{1}{(\nu - \nu_0(i))^2 + \Delta\nu_{\text{short}}^2(i)} & \text{for } \nu \geq \nu_0(i) \\ \frac{2}{1 + \Delta\nu_{\text{short}}(i)/\Delta\nu_{\text{long}}(i)} \frac{\Delta\nu_{\text{long}}(i)}{\pi} \frac{1}{(\nu - \nu_0(i))^2 + \Delta\nu_{\text{long}}^2(i)} & \text{for } \nu < \nu_0(i) \end{cases} \quad (4)$$

For each band, the free parameters are $I_{\text{band}}(i)$, $\nu_0(i)$, $\Delta\nu_{\text{short}}(i)$ and $\Delta\nu_{\text{long}}(i)$. The profile can be fixed, then the only parameter is $I_{\text{band}}(i)$.

5. We assume a foreground slab extinction, with two components: dust and ices. Those component vary independently. The free parameters are the A_V of each component. The wavelength dependent absorption probability is:

$$P_{\text{abs}}(\nu) = \exp \left(-A_V^{\text{dust}} A_{\text{dust}}(\nu) - A_{15.2 \mu\text{m}}^{CO_2} A_{CO_2}(\nu) \right), \quad (5)$$

where $A_{\text{dust}}(\nu)$ is the wavelength dependent optical depth of the standard dust composition (silicate, graphite), normalised to A_V , and $A_{CO_2}(\nu)$ is the wavelength dependent optical depth of CO₂ ices (White et al., 2009, at 75 K), normalised at 15.2 μm.

The total model is then fit to the observed spectrum by minimizing the χ^2 . The total mode is:

$$F_\nu^{\text{model}}(\nu) = \left(F_\nu^*(\nu) + \sum_{i=1}^{N_{\text{grain}}} F_\nu^{\text{grain}}(\nu; i) + \sum_{i=1}^{N_{\text{band}}} F_\nu^{\text{band}}(\nu; i) \right) \times P_{\text{abs}}(\nu) + \sum_{i=1}^{N_{\text{line}}} F_\nu^{\text{line}}(\nu; i). \quad (6)$$

1.3 Calibration of the Aromatic Feature Profiles

We calibrate the PAH feature parameters in the 5 to 20 μm range.

- To fix the profiles of the aromatic band, we first fit the ISO/SWS spectrum of the red rectangle, in order to calibrate the narrow bands (Fig. 2). The plateaux of this region are not prominent. Those will be fit in the second step.

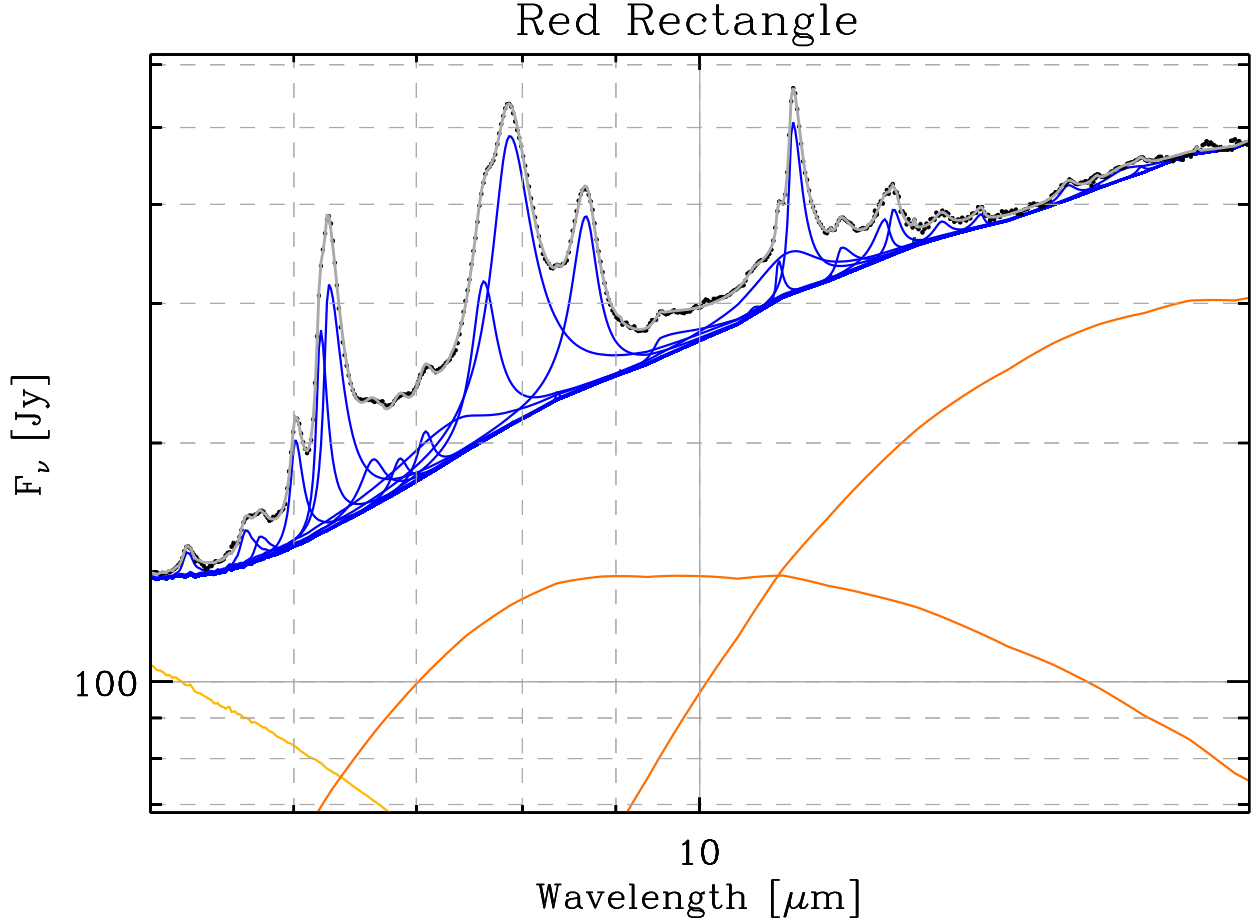


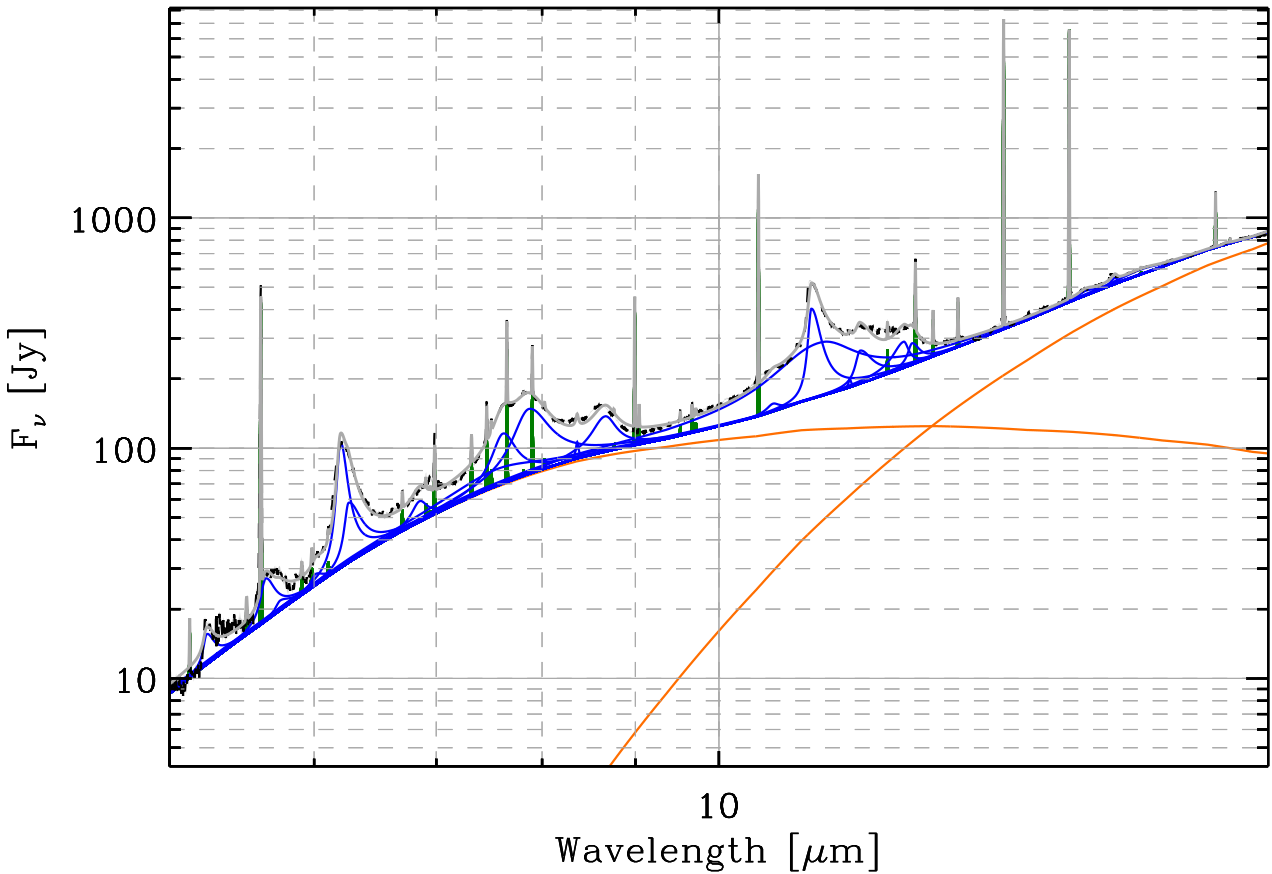
Figure 2: Calibration of the band profile on the Red Rectangle.

- Then, the narrow band profile is used as a basis to fit the ISO/SWS spectrum of NGC 7027 (Fig. 3). We derive the plateau of the 8 μm and 12 μm complexes from this fit. The 17 μm complex is too weak to do so.
- Moreover, the 8.6 μm features is off-centered. Since the sources of the LMC are more of the type of NGC 7027, we let this feature free to vary and adopt this new profile.
- Finally the 17 μm complex is fit from the IRS spectrum of M 17 (Galliano et al., 2010, position 2), taking into account foreground extinction.

The final band parameters are shown in Table 3 and on Fig. 7. In Table 3, the parameters refer conveniently to the wavelength, although the band is parametrised by the frequency. The transformation is the following:

$$\left\{ \begin{array}{l} \nu_0 = \frac{c}{\lambda_0} \\ \Delta\nu_{\text{short}} = \frac{c}{\lambda_0 - \Delta\lambda_{\text{short}}} - \frac{c}{\lambda_0} \\ \Delta\nu_{\text{long}} = \frac{c}{\lambda_0} - \frac{c}{\lambda_0 + \Delta\lambda_{\text{long}}}. \end{array} \right. \quad (7)$$

NGC 7027



NGC 7027

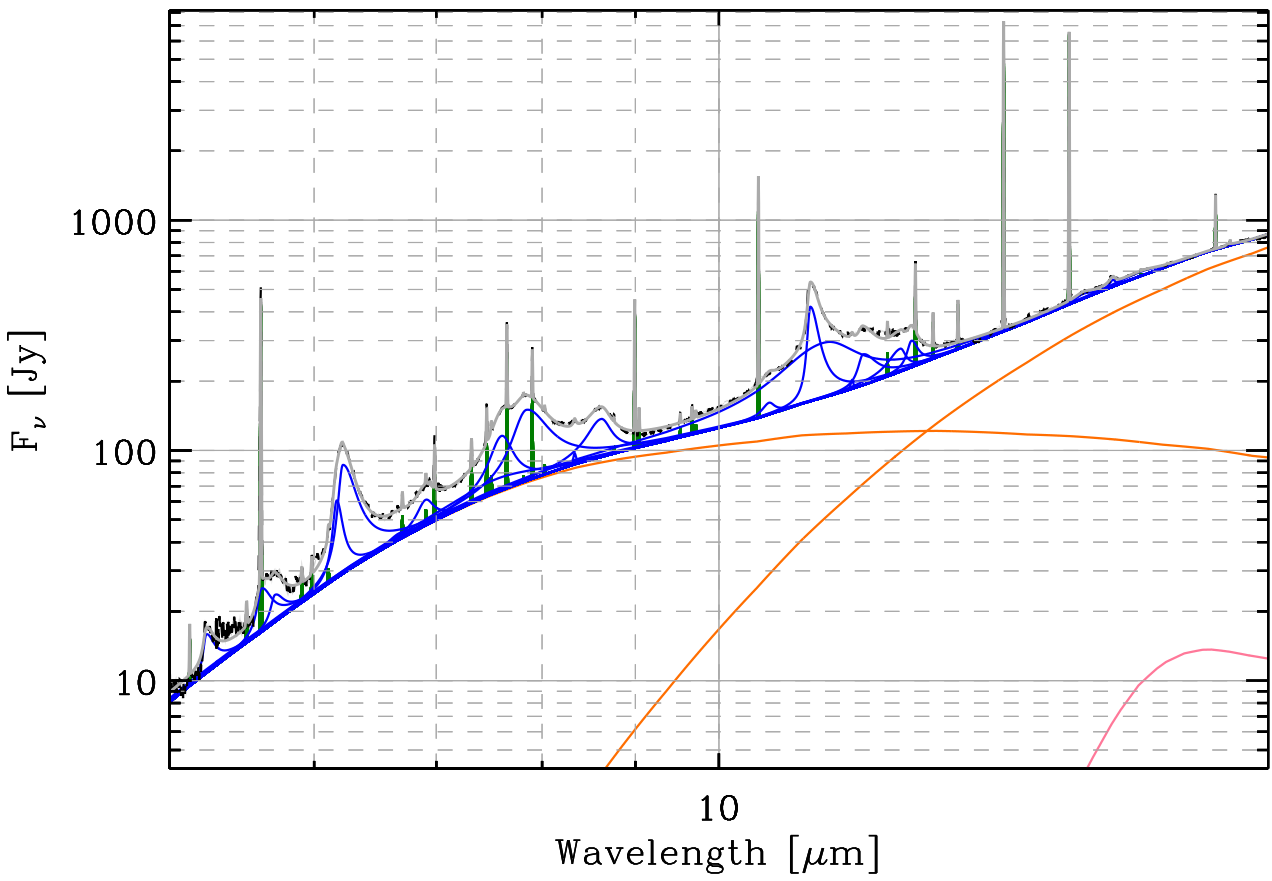


Figure 3: Calibration of the band profile on NGC 7027. The top panel shows the fit, fixing the narrow features to the parameters derived from the Red Rectangle. The bottom panel shows the fit letting the widths vary by 10 %.

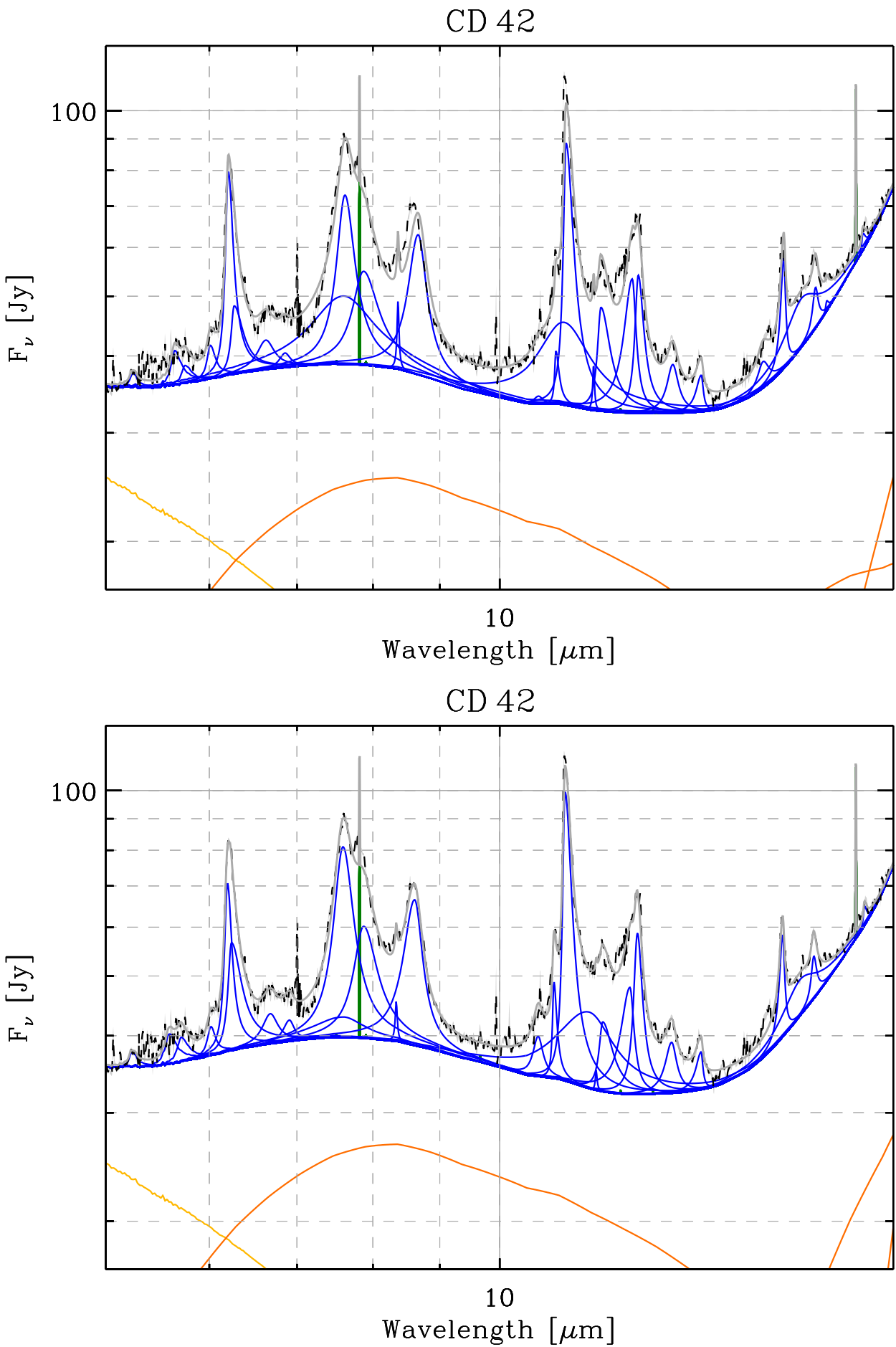


Figure 4: Calibration of the band profile on CD 42. The top panel shows the fit, fixing the narrow features to the parameters derived from the Red Rectangle. The bottom panel shows the fit letting the widths vary by 10 %.

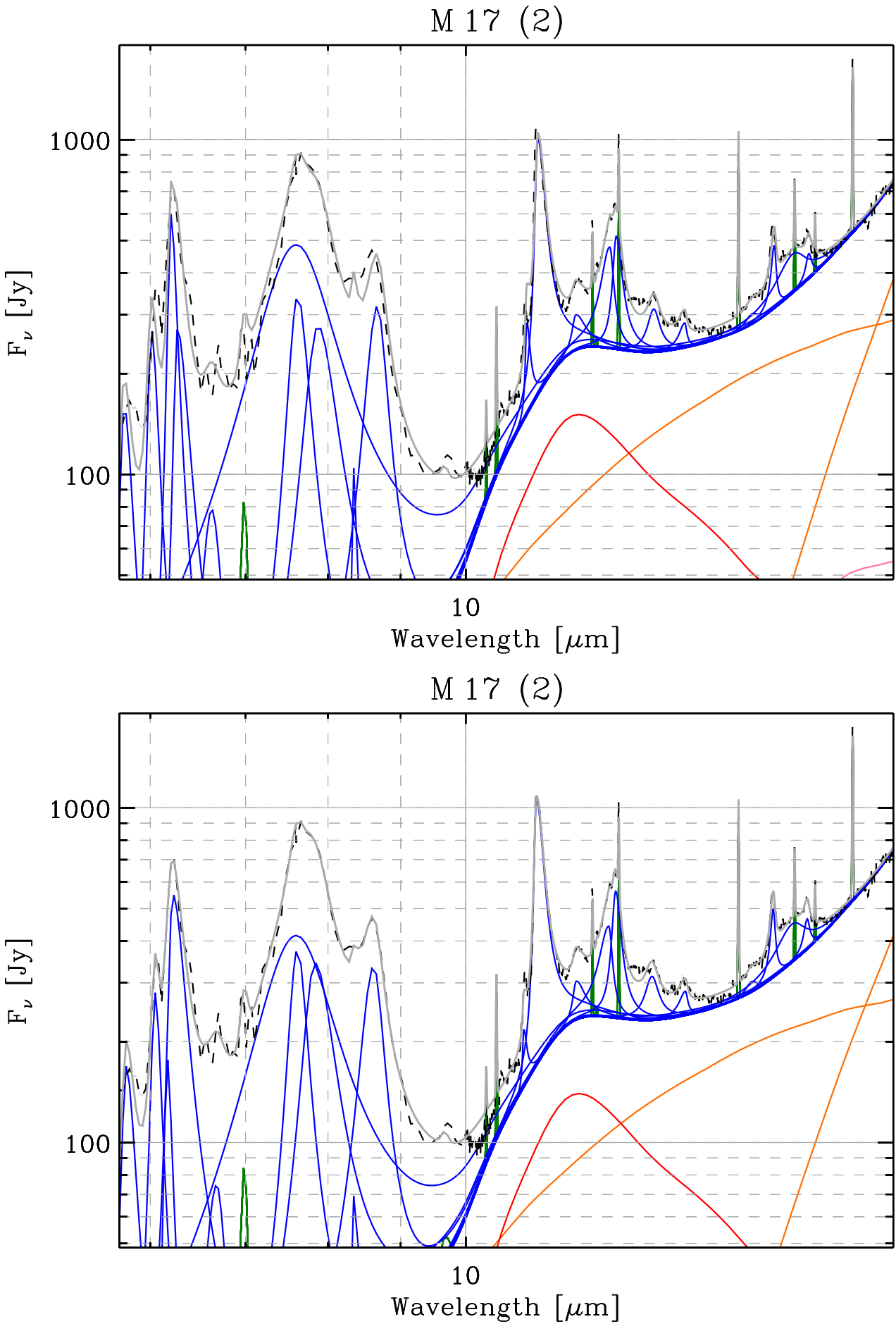


Figure 5: Calibration of the band profile on M 17, with a corundum component. The top panel shows the fit, fixing the narrow features to the parameters derived from the Red Rectangle. The bottom panel shows the fit letting the widths vary by 10%.

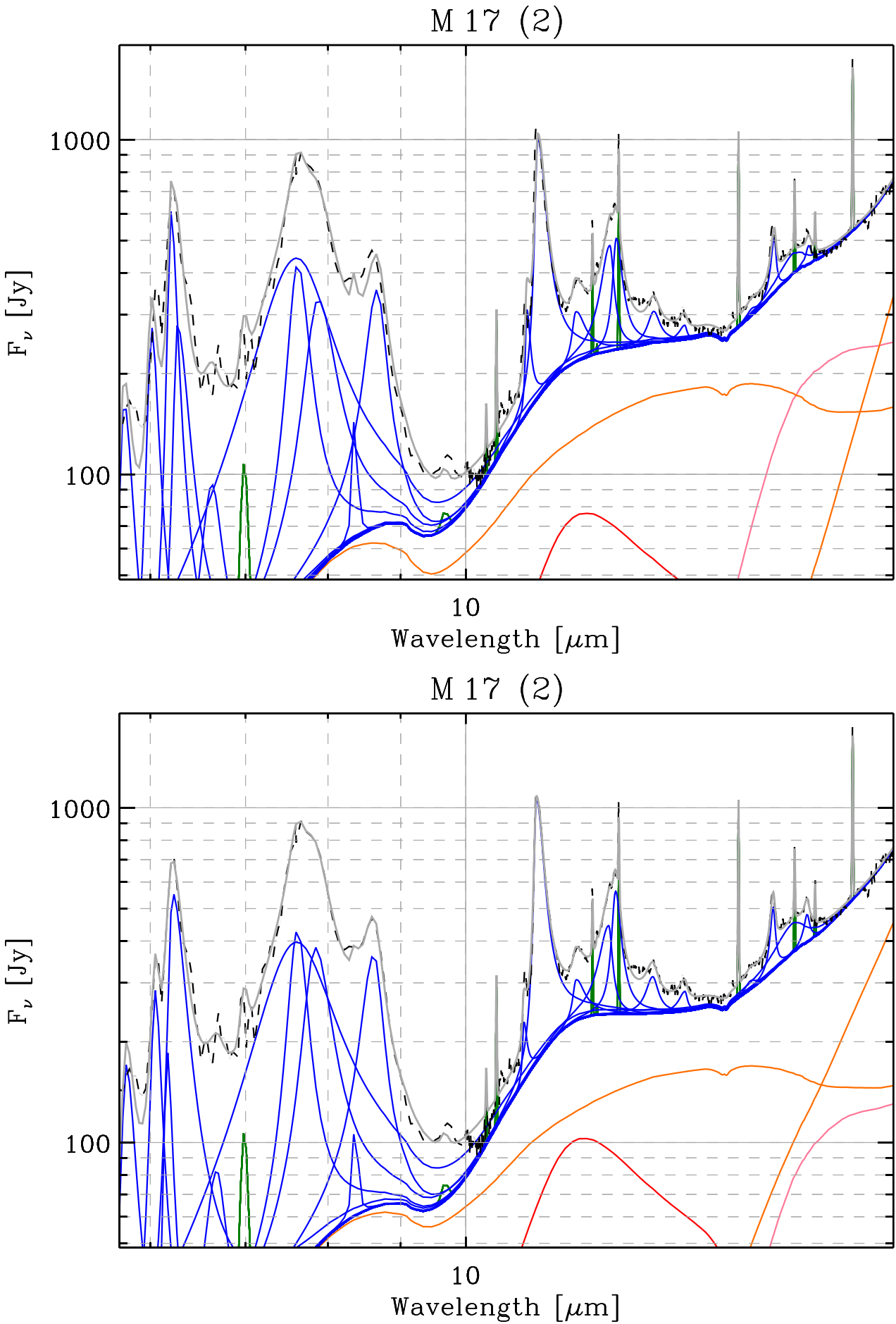


Figure 6: Calibration of the band profile on M 17, with a corundum component. The top panel shows the fit, fixing the narrow features to the parameters derived from the Red Rectangle. The bottom panel shows the fit letting the widths vary by 10%.

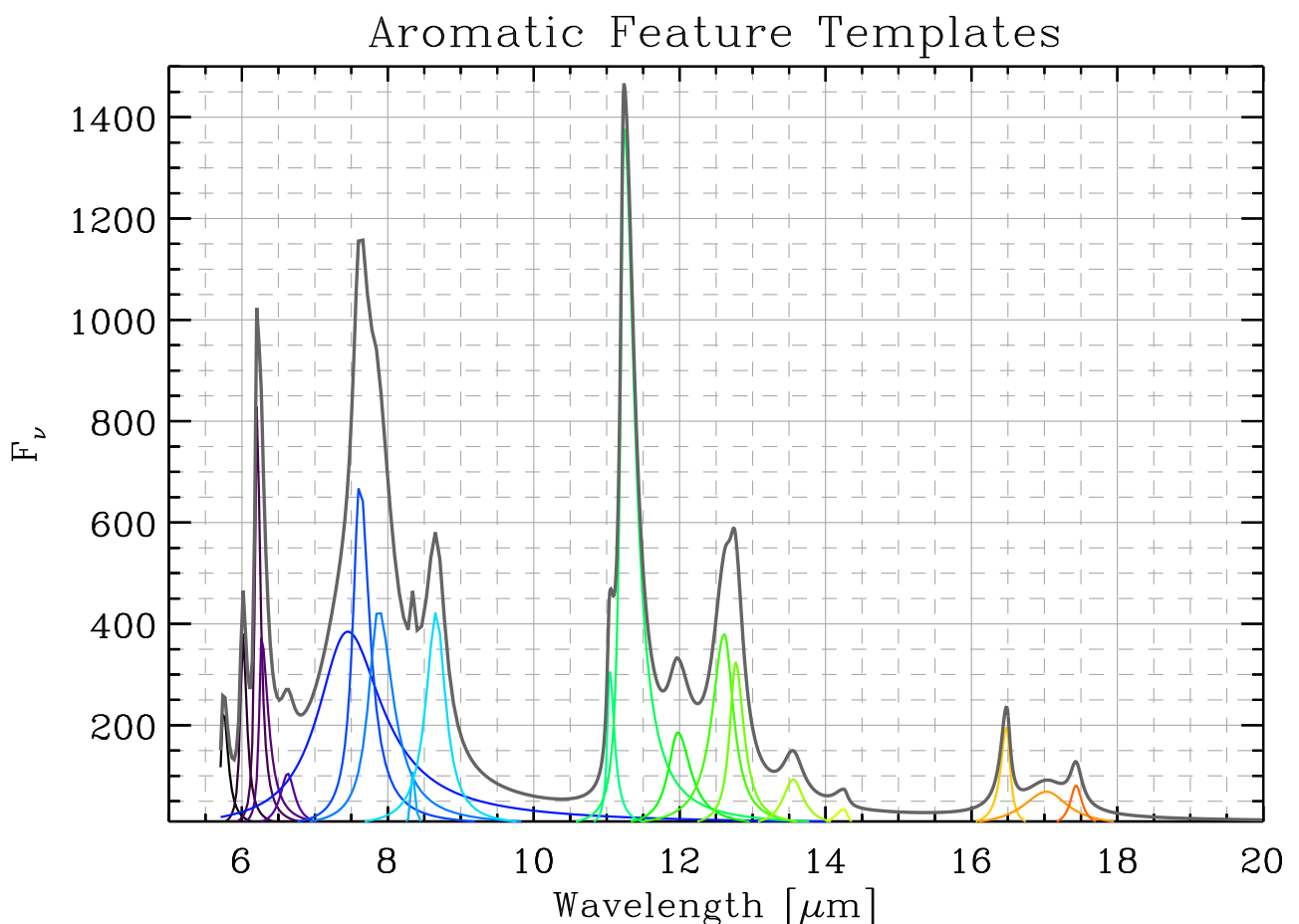


Figure 7: Calibrated aromatic feature profiles.

λ_0 [μm]	$\Delta\lambda_{\text{short}}$ [μm]	$\Delta\lambda_{\text{long}}$ [μm]	Input Code Label
5.2395	0.0252	0.0583	Small 5.2
5.6437	0.0400	0.0800	Small 5.7 (1)
5.7490	0.0400	0.0800	Small 5.7 (2)
6.0107	0.0400	0.0666	Small 6.0
6.2034	0.0313	0.0600	Main 6.2 (1)
6.2673	0.0369	0.1163	Main 6.2 (2)
6.6274	0.1200	0.1200	Small 6.6
6.8549	0.0800	0.0800	Small 6.8
7.0792	0.0800	0.0800	Small 7.1
7.6000	0.4800	0.5025	Plateau 7.7
7.6171	0.1186	0.1453	Main 7.7 (1)
7.8705	0.1700	0.2452	Main 7.7 (2)
8.3624	0.0163	0.0163	Small 8.3
8.6205	0.1834	0.1334	Main 8.6
9.5245	0.1077	0.6000	Small 9.5
10.7071	0.1000	0.1000	Small 10.7
11.0383	0.0270	0.0731	Small 11.0
11.2379	0.0535	0.1525	Main 11.2
11.4004	0.7200	0.6366	Plateau 11.3
11.7964	0.0208	0.0208	Small 11.8
11.9497	0.0804	0.2219	Small 11.9
12.6268	0.2000	0.0944	Main 12.7 (1)
12.7603	0.0804	0.1400	Main 12.7 (2)
13.5593	0.1595	0.1605	Small 13.6
14.2571	0.1521	0.0590	Small 14.2
15.8931	0.1786	0.2000	Small 15.6
16.4829	0.1000	0.0585	Small 16.4
17.0829	0.4978	0.5612	Plateau 17.0
17.4285	0.1000	0.1000	Small 17.4
17.7711	0.0308	0.0752	Small 17.8
18.9256	0.0346	0.1157	Small 18.9

Table 3: Calibrated aromatic band parameters.

2 Application

2.1 The Calling sequence

```
MILES, wavOBS[N], FnuOBS[N] [Nx,Ny,N], dFnuOBS[N] [Nx,Ny,N], INSTRUMENT=[N],
WEIGHTS=[N] [Nx,Ny,N], MASK=mask[Nx,Ny],
(wave in microns is supposed to be sorted, Fnu in Jy)
COPY=fileps, /PDF, /EPS, SAVE=filexdr, /MODELSAVE, /NOPLOT, /LOGPLOT, /QUIET,
TITLE='' [Nx,Ny]], /MILLI, RANGEWAVELENGTH=[,], /HIGHRES, FTOL=1.D-5,
NITER=250, /RESTART, /COPLINE
(Physical components)
BBTYPE={1,['crb','gra','sil_norm','al2o3_koike',etc.]},
LINES={1,['[ArIII]','[SIV]',etc.]},
BANDS={1,['PAH6.2','PAH7.4',etc.]},
EXTINCTION={1,['Dudley','CO2']},
LINE_FIRST={1,['[ArIII]',etc.]},
(BB parameters)
TEMPBB=[Nbb], FIXTEMPBB={1,[Nbb]}, TMINBB={T,[Nbb]}, TMAXBB={T,[Nbb]},
(Field stars)
MASSSTAR=, /FIXMASSSTAR, RANGEMASSSTAR=[,],
(Line parameters)
FIXCENTERLINE={1,[Nline]}, FIXSIGMALINE={1,[Nline]},
(band parameters)
FIXCENTERBAND={1,[Nband]}, FIXSIGMABAND={1,[Nband]}, /UNTIESIGMABAND,
(Extinction)
Av=, /FIXAV, RANGEAV=[,],
(Outputs)
PARSTR=, ERRPARSTR=, PARINFO=, FIT=, STATUS=, CHI2=, BAND_STRUCTURE=bandIN,
BB_STRUCTURE=bbIN
```

2.2 Error Analysis

We subdivided our sample into several classes of spectra based on the intensities of the $7.7\mu\text{m}$ feature and of the continuum. Fig. 8 show these classes of spectra.

We compute Monte-Carlo errors for each of these spectra.

References

- Begemann, B., Dorschner, J., Henning, T., et al. 1997, *ApJ*, **476**, 199
Bernard Salas, J., Pottasch, S. R., Beintema, D. A., & Wesselius, P. R. 2001, *A&A*, **367**, 949
Fioc, M. & Rocca-Volmerange, B. 1997, *A&A*, **326**, 950
Galliano, F., Hony, S., Madden, S. C., et al. 2010, *A&A*, *in prep.*
Jäger, C., Dorschner, J., Mutschke, H., Posch, T., & Henning, T. 2003, *A&A*, **408**, 193
Koike, C., Kaito, C., Yamamoto, T., et al. 1995, *Icarus*, **114**, 203
Laor, A. & Draine, B. T. 1993, *ApJ*, **402**, 441
Rouleau, F. & Martin, P. G. 1991, *ApJ*, **377**, 526
Weingartner, J. C. & Draine, B. T. 2001, *ApJ*, **548**, 296
White, D. W., Gerakines, P. A., Cook, A. M., & Whittet, D. C. B. 2009, *ApJS*, **180**, 182

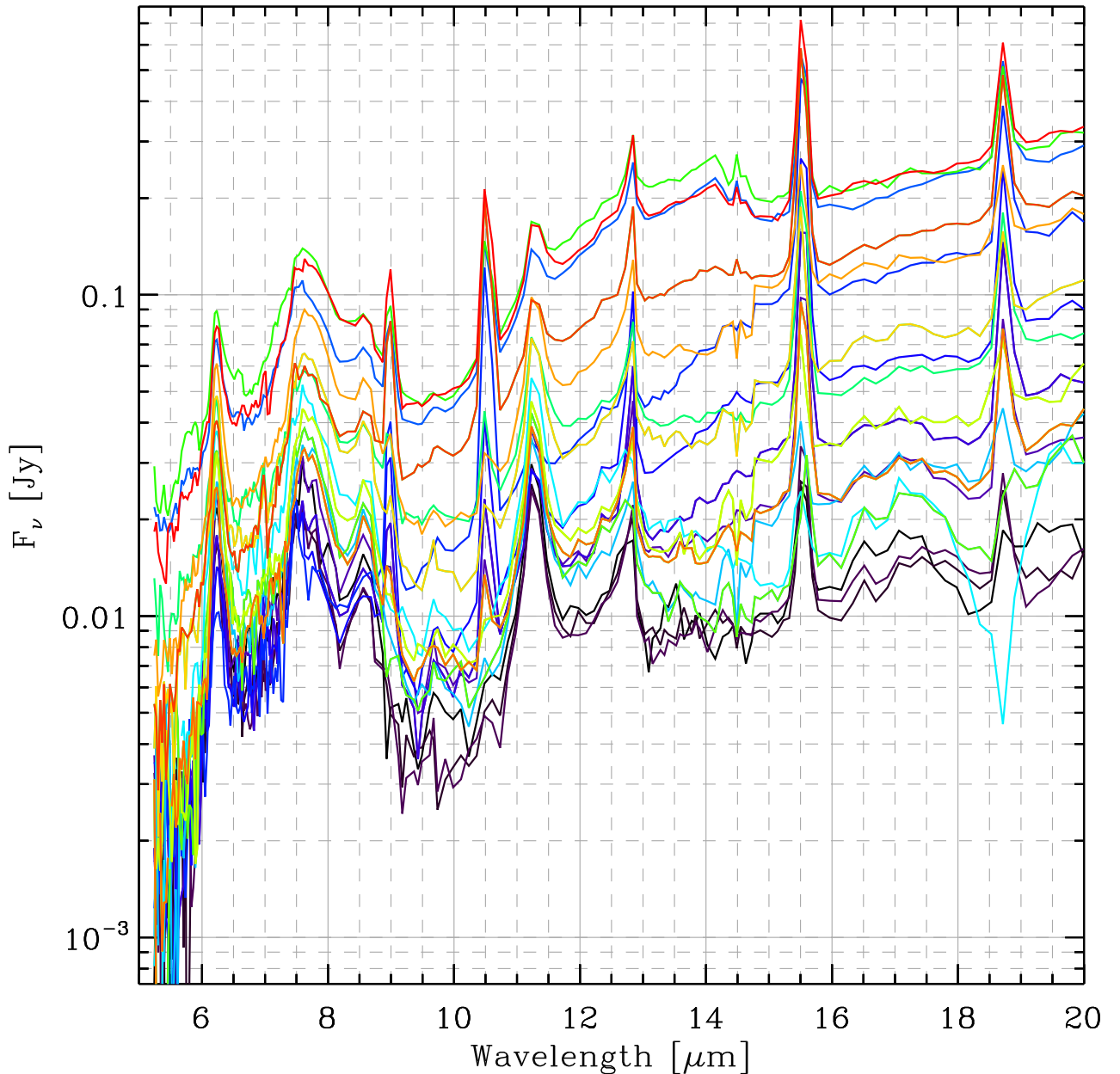


Figure 8: Various classes of spectra defined for the error estimate.

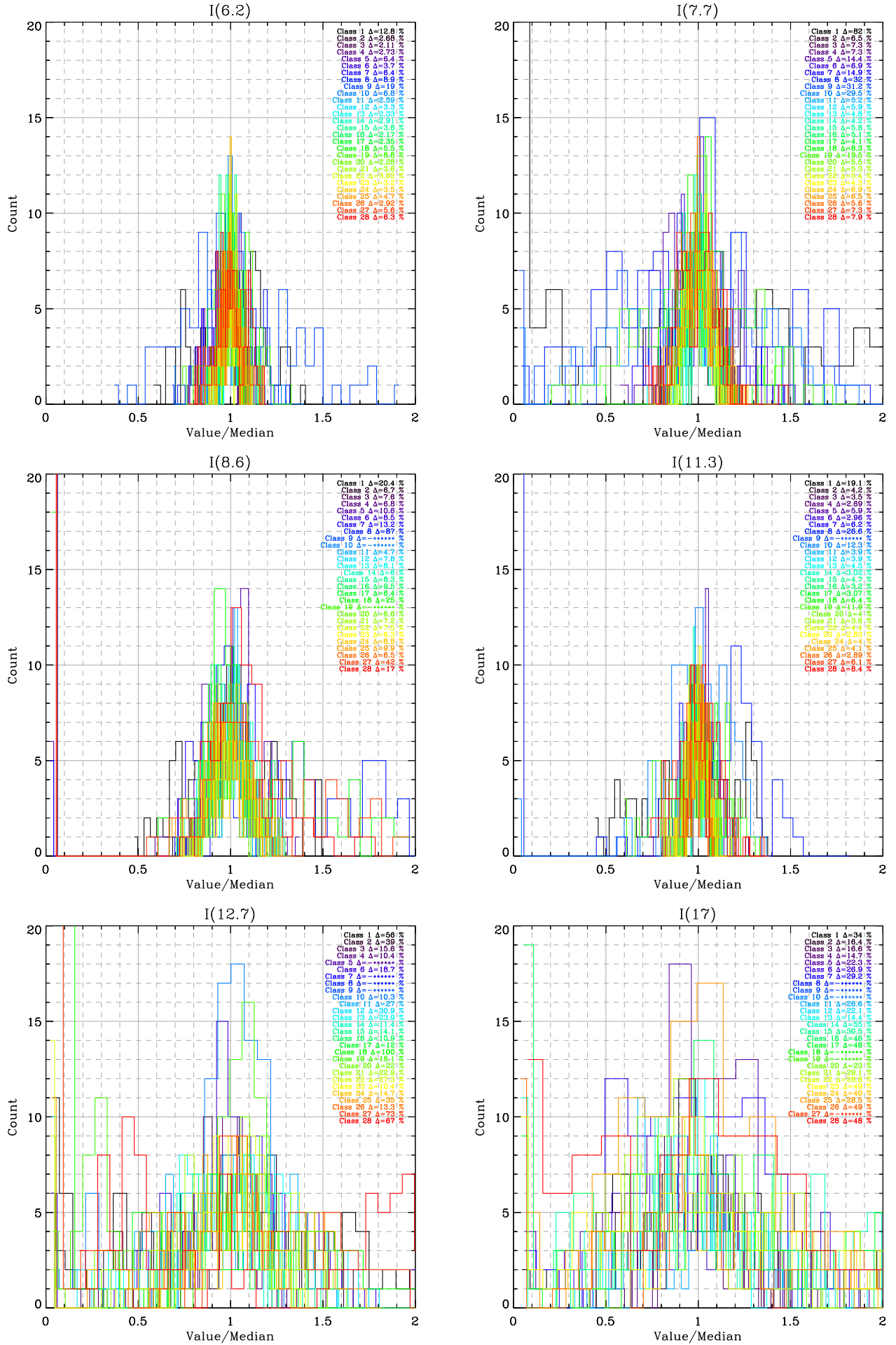


Figure 9: Statistical distributions of the main feature intensities.

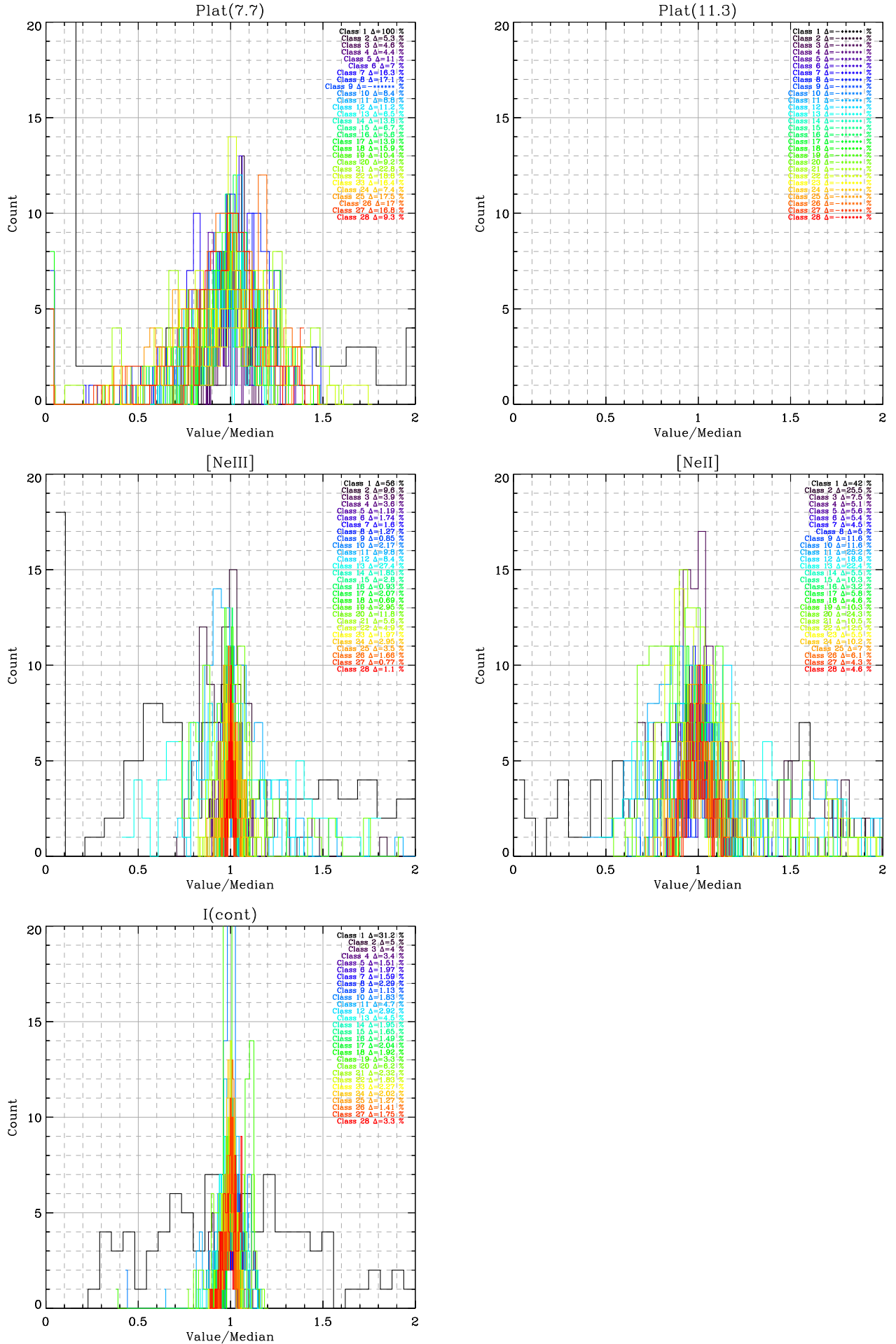


Figure 10: Statistical distributions of the main feature intensities.

Class		I _{6.2}	I _{7.7}	I _{8.6}	I _{11.3}	I _{12.7}	Comp ₁₇ [10 ⁻¹⁵ W m ⁻²]	Plat _{7.7}	[NeIII]	[NeII]	I _{cont}	Comp _{7.7}	CompCor _{11.3}
(1) faint	$\langle \cdot \rangle$	0.0194	0.006	0.0171	0.0155	0.0054	0.0054	0.0065	0.00075	0.0035	0.0253	0.0146	0.0173
	$\sigma(\cdot)$	0.0025	0.0049	0.0035	0.00296	0.00302	0.00182	0.0065	0.00042	0.00148	0.0079	0.0061	0.00242
(2) fb_f1_ff	$\langle \cdot \rangle$	0.47	0.46	0.255	0.289	0.062	0.137	1.05	0.045	0.042	0.77	1.51	0.39
	$\sigma(\cdot)$	0.0126	0.0296	0.0172	0.0123	0.0239	0.0224	0.056	0.0043	0.0107	0.038	0.035	0.0289
(3) fb_f1_mf	$\langle \cdot \rangle$	0.36	0.299	0.191	0.248	0.064	0.057	0.88	0.046	0.042	0.81	1.18	0.38
	$\sigma(\cdot)$	0.0077	0.022	0.0145	0.0087	0.01	0.0095	0.04	0.0018	0.0032	0.033	0.022	0.039
(4) fb_f1_bf	$\langle \cdot \rangle$	0.34	0.307	0.183	0.242	0.058	0.075	0.91	0.059	0.049	0.81	1.22	0.38
	$\sigma(\cdot)$	0.0093	0.0224	0.0125	0.0065	0.006	0.011	0.04	0.00213	0.00251	0.028	0.0227	0.036
(5) fb_ml_ff	$\langle \cdot \rangle$	0.38	0.38	0.224	0.238	0	0.033	0.86	0.33	0.13	2.47	1.23	0.48
	$\sigma(\cdot)$	0.0241	0.054	0.0238	0.0141	0	0.0075	0.095	0.0039	0.0073	0.037	0.075	0.057
(6) fb_ml_mf	$\langle \cdot \rangle$	0.47	0.4	0.276	0.35	0.062	0.082	0.94	0.205	0.104	1.85	1.52	0.59
	$\sigma(\cdot)$	0.0175	0.041	0.0234	0.0103	0.0116	0.022	0.066	0.0036	0.0056	0.037	0.047	0.044
(7) fb_ml_bf	$\langle \cdot \rangle$	0.37	0.41	0.215	0.231	0	0.0314	0.79	0.33	0.131	2.5	1.19	0.45
	$\sigma(\cdot)$	0.0235	0.061	0.0284	0.0143	0	0.0092	0.129	0.0053	0.0059	0.04	0.07	0.058
(8) fb_b1_ff	$\langle \cdot \rangle$	0.303	0.249	0.137	0.152	0	0	0.76	0.53	0.238	4.1	0.99	0.32
	$\sigma(\cdot)$	0.027	0.079	0.119	0.04	0	0	0.13	0.0067	0.012	0.094	0.091	0.166
(9) fb_b1_mf	$\langle \cdot \rangle$	0.179	0.315	0	0	0	0	0	0.93	0.132	7.5	0.37	0.0104
	$\sigma(\cdot)$	0.034	0.098	0	0	0	0	0	0.008	0.0152	0.085	0.108	0.0104
(10) fb_b1_bf	$\langle \cdot \rangle$	1.27	0.89	0	0.69	0.87	0	5.5	0.93	0.263	16.3	6.3	0.75
	$\sigma(\cdot)$	0.086	0.261	0	0.085	0.09	0	0.46	0.0202	0.0304	0.297	0.292	0.094
(11) mb_f1_ff	$\langle \cdot \rangle$	0.74	0.95	0.39	0.43	0.095	0.166	1.03	0.036	0.052	1.05	1.99	0.61
	$\sigma(\cdot)$	0.0191	0.049	0.018	0.0169	0.0255	0.044	0.091	0.0035	0.0132	0.049	0.063	0.047
(12) mb_f1_mf	$\langle \cdot \rangle$	0.54	0.89	0.32	0.34	0.068	0.141	0.94	0.042	0.053	1.41	1.82	0.46
	$\sigma(\cdot)$	0.0176	0.053	0.0251	0.0135	0.021	0.0312	0.106	0.0035	0.0099	0.041	0.076	0.058
(13) mb_f1_bf	$\langle \cdot \rangle$	0.84	1.1	0.43	0.51	0.122	0.167	1.62	0.042	0.064	1.44	2.72	0.93
	$\sigma(\cdot)$	0.0196	0.053	0.035	0.023	0.029	0.024	0.105	0.0116	0.0145	0.065	0.062	0.049
(14) mb_ml_ff	$\langle \cdot \rangle$	0.53	0.92	0.314	0.36	0.092	0.069	0.65	0.165	0.08	1.79	1.58	0.5
	$\sigma(\cdot)$	0.0153	0.039	0.0189	0.0109	0.0105	0.038	0.09	0.00307	0.0044	0.035	0.071	0.057
(15) mb_ml_mf	$\langle \cdot \rangle$	0.99	1.32	0.57	0.68	0.208	0.226	2.6	0.261	0.12	4.3	3.9	0.98
	$\sigma(\cdot)$	0.036	0.077	0.048	0.032	0.0295	0.069	0.174	0.0073	0.0123	0.07	0.122	0.119
(16) mb_ml_bf	$\langle \cdot \rangle$	0.76	1.01	0.48	0.57	0.146	0.0184	2.17	0.38	0.135	4.7	3.2	0.98
	$\sigma(\cdot)$	0.0165	0.051	0.046	0.0184	0.016	0.0084	0.122	0.0036	0.0043	0.07	0.126	0.086
(17) mb_b1_ff	$\langle \cdot \rangle$	0.53	0.94	0.313	0.36	0.091	0.067	0.63	0.164	0.081	1.79	1.58	0.5
	$\sigma(\cdot)$	0.0124	0.039	0.0199	0.0111	0.0109	0.032	0.088	0.0034	0.0046	0.036	0.069	0.044
(18) mb_b1_mf	$\langle \cdot \rangle$	0.77	1.18	0.45	0.52	0.088	0	1.99	0.95	0.284	11.5	3.2	1.66
	$\sigma(\cdot)$	0.043	0.098	0.113	0.033	0.088	0	0.316	0.0065	0.0132	0.22	0.296	0.26
(19) mb_b1_bf	$\langle \cdot \rangle$	1.6	1.54	0	0.88	1.08	0	7.1	0.81	0.32	18.7	8.5	1.02
	$\sigma(\cdot)$	0.141	0.302	0	0.105	0.173	0	0.74	0.024	0.033	0.62	0.44	0.166
(20) bb_f1_ff	$\langle \cdot \rangle$	0.88	0.95	0.39	0.45	0.098	0.164	1.03	0.038	0.051	1.05	1.99	0.61
	$\sigma(\cdot)$	0.0167	0.052	0.026	0.0169	0.0216	0.038	0.095	0.0045	0.0124	0.066	0.061	0.046
(21) bb_f1_mf	$\langle \cdot \rangle$	0.69	1.32	0.43	0.45	0.094	0.064	0.75	0.087	0.065	2.21	2.08	0.48
	$\sigma(\cdot)$	0.0245	0.069	0.0307	0.0164	0.0216	0.0186	0.171	0.0049	0.0068	0.051	0.125	0.048
(22) bb_f1_bf	$\langle \cdot \rangle$	0.69	1.32	0.42	0.45	0.095	0.068	0.73	0.087	0.067	2.23	2.04	0.49
	$\sigma(\cdot)$	0.0207	0.071	0.032	0.0196	0.026	0.0197	0.137	0.0043	0.0084	0.041	0.096	0.053
(23) bb_ml_ff	$\langle \cdot \rangle$	0.53	0.94	0.32	0.36	0.092	0.067	0.64	0.165	0.08	1.8	1.58	0.5
	$\sigma(\cdot)$	0.0172	0.04	0.0201	0.0103	0.0095	0.033	0.105	0.0033	0.0044	0.041	0.068	0.05
(24) bb_ml_mf	$\langle \cdot \rangle$	1	1.32	0.59	0.69	0.211	0.229	2.64	0.262	0.119	4.2	4	0.97
	$\sigma(\cdot)$	0.035	0.091	0.052	0.0277	0.0309	0.092	0.196	0.0077	0.0122	0.085	0.133	0.138
(25) bb_ml_bf	$\langle \cdot \rangle$	1.22	2.32	0.8	0.86	0.204	0.08	2.47	0.32	0.204	8.1	4.7	1.63
	$\sigma(\cdot)$	0.058	0.152	0.078	0.035	0.072	0.0227	0.43	0.0113	0.0143	0.102	0.33	0.276
(26) bb_b1_ff	$\langle \cdot \rangle$	0.53	0.93	0.309	0.36	0.093	0.068	0.64	0.164	0.08	1.81	1.57	0.48
	$\sigma(\cdot)$	0.0155	0.052	0.02	0.0103	0.0123	0.034	0.109	0.00273	0.0049	0.0255	0.056	0.053
(27) bb_b1_mf	$\langle \cdot \rangle$	0.79	1.18	0.45	0.51	0.15	0	2	0.95	0.287	11.4	3.2	1.55
	$\sigma(\cdot)$	0.045	0.086	0.19	0.0313	0.109	0	0.34	0.0073	0.0124	0.2	0.32	0.33
(28) bb_b1_bf	$\langle \cdot \rangle$	1.4	2.52	0.96	1.03	0.52	0.119	5	1.19	0.43	17.6	7.4	3.2
	$\sigma(\cdot)$	0.089	0.2	0.163	0.086	0.35	0.057	0.46	0.0132	0.0198	0.59	0.34	1.96

Table 4: Relative error of the main features for each class of spectrum.